Development 138, 3189-3198 (2011) doi:10.1242/dev.063073

LATE MERISTEM IDENTITY2 acts together with LEAFY to activate *APETALA1*

Jennifer J. Pastore, Andrea Limpuangthip, Nobutoshi Yamaguchi, Miin-Feng Wu, Yi Sang, Soon-Ki Han, Lauren Malaspina, Natasha Chavdaroff, Ayako Yamaguchi and Doris Wagner*

SUMMARY

The switch from producing vegetative structures (branches and leaves) to producing reproductive structures (flowers) is a crucial developmental transition that significantly affects the reproductive success of flowering plants. In *Arabidopsis*, this transition is in large part controlled by the meristem identity regulator LEAFY (LFY). The molecular mechanisms by which LFY orchestrates a precise and robust switch to flower formation is not well understood. Here, we show that the direct LFY target *LATE MERISTEM IDENTITY2* (*LMI2*) has a role in the meristem identity transition. Like LFY, LMI2 activates *AP1* directly; moreover, LMI2 and LFY interact physically. LFY, LMI2 and AP1 are connected in a feed-forward and positive feedback loop network. We propose that these intricate regulatory interactions not only direct the precision of this crucial developmental transition in rapidly changing environmental conditions, but also contribute to its robustness and irreversibility.

KEY WORDS: APETALA1, LEAFY, LMI2, Meristem identity transition, Reproductive development, *Arabidopsis*

INTRODUCTION

Flowering plants transition through a number of distinct developmental phases in their lifecycle. During each phase, different organs are generated from a group of cells at the flanks of the shoot apical meristem, which form the primordia (Steeves and Sussex, 1989). Developmental phase transitions have been studied extensively in the plant model system *Arabidopsis thaliana* (Araki, 2001; Blazquez et al., 2006; Poethig, 2003; Steeves and Sussex, 1989). During the vegetative phase, the primordia give rise to a series of leaves, which form the basal rosette. During the early reproductive phase, the shoot apical meristem grows upward (bolts) and the newly formed primordia develop into secondary inflorescence branches subtended by cauline leaves. Finally, after the meristem identity transition, the first flowers are formed.

The precise timing of flower formation is crucial for reproductive fitness, as plants must ensure that the energy and resources accumulated during the vegetative phase are optimally allocated to the production of offspring (Roux et al., 2006). Plants rely on both environmental and endogenous cues to fine-tune the onset of reproductive development (Araki, 2001; Koornneef et al., 1998; Simpson et al., 1999). These signals modulate the level and activity of flowering-time regulators, which initiate the reproductive phase and induce expression of the meristem identity genes (Amasino, 2010; Baurle and Dean, 2006; Kobayashi and Weigel, 2007; Komeda, 2004; Turck et al., 2008). The meristem identity regulators then trigger formation of the first flower (Blazquez et al., 2006; Liu et al., 2009a; Parcy, 2005).

Two key meristem identity regulators in *Arabidopsis* are the plant-specific transcription factor LEAFY (LFY) and the MADS box transcription factor APETALA1 (AP1). LFY is considered to be a central meristem identity regulator because *lfy* null mutants cause a very dramatic delay in the meristem identity transition (Huala and Sussex, 1992; Weigel et al., 1992). Moreover, *LFY* upregulation in the initiating primordia flanking the shoot apical meristem is one of the first steps in the regulatory cascade that leads to the meristem identity transition (Blazquez et al., 1997; Hempel et al., 1997). LFY executes its meristem identity role in part by activating *AP1* expression directly (Parcy et al., 1998; Wagner et al., 1999; William et al., 2004). *AP1* upregulation marks commitment to flower formation (Blazquez et al., 1997; Bowman et al., 1993; Hempel et al., 1997; Liu et al., 2007; Mandel and Yanofsky, 1995; Yu et al., 2004). AP1 promotes floral fate by upregulating floral identity pathways and by repressing inflorescence identity pathways (Ferrandiz et al., 2000; Kaufmann et al., 2010; Liljegren et al., 1999; Liu et al., 2007; Yu et al., 2004). Two LFY-independent pathways can also upregulate *AP1*: one involves the photoperiod flowering-time regulators, FLOWERING LOCUS T (FT) and FD, and the other involves components of the age-sensing flowering-time pathway, the SBP transcription factors (Abe et al., 2005; Wang et al., 2009; Wigge et al., 2005; Yamaguchi et al., 2009). In agreement with this, simultaneous loss-of-function mutations in both *LFY* and *AP1* results in plants that essentially lack flowers (Bowman et al., 1993; Huala and Sussex, 1992; Schultz and Haughn, 1993; Weigel et al., 1992).

Although the meristem identity transition is a key developmental switch, our understanding of the events that lead from *LFY* upregulation to flower formation is still incomplete. Previously, we used a genomic approach to define direct targets of LFY during the meristem identity transition (William et al., 2004). This approach identified the meristem identity regulators and direct LFY targets *CAULIFLOWER* (*CAL*), a close AP1 homolog, and *LATE MERISTEM IDENTITY1* (*LMI1*), a class I HD-Zip transcription factor (Saddic et al., 2006; William et al., 2004). Another direct LFY target identified was AtMYB17 (William et al., 2004). AtMYB17 is a member of the R2R3 class of MYB transcription factors, which have important roles in many processes in plants, including cell fate specification, metabolism, and biotic and abiotic

Department of Biology, University of Pennsylvania, School of Arts and Sciences, Philadelphia, PA 19104, USA.

*Author for correspondence (wagnerdo@sas.upenn.edu)

Accepted 19 May 2011

stress responses (Dubos et al., 2010; Kranz et al., 1998; Martin and Paz-Ares, 1997; Stracke et al., 2001). The *Arabidopsis* homologs of AtMYB17, AtMYB16 (MIXTA) and AtMYB106 (NOECK), have been reported to function in the determination of cell shape in the petal epidermis and in the repression of trichome branching (Baumann et al., 2007; Jakoby et al., 2008). The biological function of AtMYB17 is not understood. Here, we show a role for AtMYB17 in the meristem identity transition upstream of *AP1*; based on these findings, we renamed this gene *LATE MERISTEM IDENTITY2* (*LMI2*).

MATERIALS AND METHODS

Plant lines, growth and *LMI2* rescue construct

T-DNA insertion lines were obtained from the SALK collection (Alonso and Stepanova, 2003) and twice backcrossed to Columbia (wild type). *lfy* and *ap1* alleles used were described previously (Saddic et al., 2006; Yamaguchi et al., 2009). *lfy-2* and *lfy-10* carry the same lesion (Schultz and Haughn, 1993; Weigel et al., 1992) and were used interchangeably. For all genotyping primers, see Table S2 in the supplementary material.

All plant growth was in inductive photoperiod. Seeds were stratified for seven days at 4°C and either grown in white fluorescent lights at 22°C in soil in long-day conditions (16 hours light, 8 hours dark; 110 μmol/m^{2}s) for experiments involving phenotyping and inflorescences, or on plates (0.5× MS media) in long-day conditions for three days followed by growth in continuous light (90 μmol/m^{2}s) for seedling experiments.

For genomic rescue, the *LMI2* locus including 2150 bp upstream of the translational start site was PCR amplified, sequenced and Gateway cloned into pGWB1 (Nakagawa et al., 2007). The resulting construct was transformed into *lmi2-2 lfy-10* plants. A representative pLMI2:LMI2 *lmi2-2 lfy-10* transgenic line was characterized further. For all cloning primers see Table S3 in the supplementary material.

Semi-quantitative and quantitative PCR

Developmental age was determined based on number of days of growth and adjusted by developmental stage (emergence and size of true leaves) (Saddic et al., 2006). RNA was extracted from entire seedlings except for the study of *LMI2* mis-expression in *lmi2-1* mutants. RNA purification, reverse transcription and qRT-PCR were described previously (Yamaguchi et al., 2009). All real-time RT-PCR experiments were normalized over the ubiquitously expressed *EIF4A* gene (AT3G13920). The mean and s.e.m. were calculated for each biological replicate using three technical replicates. One representative experiment is shown. See Table S4 in the supplementary material for qRT-PCR primers used.

β-Glucuronidase (GUS) assays

Upstream and downstream intergenic regions (2150 bp upstream of the translation start site and 2699 bp downstream of the translation termination site) were PCR amplified, sequenced and cloned into pBI101 (Clontech, Mountain View, CA, USA). Wild-type plants (Col) were transformed and a representative transgenic line was characterized. To investigate the role of LFY on *LMI2:GUS* expression, LMI2:GUS was crossed to *lfy-9*, 35S:LFY-GR in L*er* (Wagner et al., 1999), and L*er* (wild type). GUS assays were performed as described by Saddic et al. and Yamaguchi et al. (Saddic et al., 2006; Yamaguchi et al., 2005) using seven-day-old seedlings or 1-2 cm bolted primary inflorescences. For transient induction assays, seven-day-old F1 seedlings (LMI2:GUS × L*er* or LMI2:GUS × 35S:LFY-GR) were incubated overnight with 10 μM dexamethasone at room temperature as previously described (Wagner et al., 1999) prior to GUS staining. Whole-mount samples and histological sections were visualized using an Olympus SZX12 dissecting or an Olympus BX51 compound microscope.

The *LMI2:GUS* reporter showed ectopic expression in the L1 layer of stems, petioles and leaves not detected by *LMI2* in situ hybridization analyses. This might be due to missing cis regulatory elements located in *LMI2* introns (Liu et al., 2007; Oh et al., 2009; Sieburth and Meyerowitz, 1997).

In situ hybridization

For the *LMI2* antisense and sense probes, the genic region downstream of the MYB DNA binding domain was used. The *AP1* in situ probe contained the genic region downstream of the MADS box. The constructs were PCR amplified, cloned into pGEM T-easy (LMI2) and pGEM-T (AP1; Promega, Madison, WI, USA), and sequenced. Sense and antisense *LMI2* probes were digested with *Sal*I and transcribed with the T7 polymerase, whereas the antisense *AP1* probe was transcribed using the T7 polymerase following digestion with *Eco*RI. The Riboprobe Combination System (Promega) and DIG RNA labeling mix (Roche, Branchburg, NJ, USA) were used for probe synthesis. In situ hybridization was performed as described by Long and Barton (Long and Barton, 1998).

Chromatin immunoprecipitation (ChIP)

The pLMI2:LMI2 rescue construct excluding the translation termination codon was Gateway cloned into pGWB13 (Nakagawa et al., 2007). pLMI2:LMI2-HA was transformed into *lmi2-2* plants followed by testing for rescue. For ChIP, 300 mg tissue from eleven-day-old seedlings of a representative line were used with 3 μg/sample or 4 μg/sample of anti-HA antibody [sc-805 (Santa Cruz, Santa Cruz, CA, USA) or 12CA5 (Roche), respectively] using published procedures (Kwon et al., 2005; William et al., 2004). LMI2 occupancy on genomic DNA was calculated by computing the enrichment over the respective input and normalized over *lmi2-2*. The mean and s.e.m. were calculated using at least three technical replicates; one representative biological replicate is shown. For ChIP-qPCR primers see Table S5 in the supplementary material.

Glutathione-S-transferase (GST) Pull-down

The LFY coding region was amplified and inserted between the *Eco*RI and *Not*I sites into pGEX-5X-1 (GE Healthcare, Piscataway, NJ, USA). The fusion protein was expressed in *Escherichia coli* (AD494). After induction with 0.1 mM IPTG at 37°C for one hour, cells were harvested by centrifugation and resuspended in ice-cold PBS containing 1 mM EDTA, 1 mM PMSF, 1 mg/ml lysozyme and 1% Triton X-100. Following a 20 minute incubation at room temperature, the cell lysate was cleared by centrifugation. Protein extracts were incubated with Sepharose 4B slurry (GE Healthcare) at 4°C for one hour. The beads were washed five times with PBS containing 1 mM EDTA and 1 mM PMSF. The protein-bound beads were used directly for pull-down assays. In vitro transcription and translation of LFY, LMI2 and NC^a (1-464 amino acid fragment of the chromatin remodeling ATPase SYD) (Wagner and Meyerowitz, 2002) and the pull-down assay were performed as previously described (Sang et al., 2005).

Yeast 2-hybrid

LMI2N consisted of the N-terminal protein coding region of LMI2, including the MYB domain and the subgroup 9 motif, whereas LMI2C contained the remainder protein coding region of LMI2. The LMI2 fragments were amplified and inserted between the *Sal*I and *Not*I sites of pDBLeu (Invitrogen, Carlsbad, CA, USA). The coding region of LFY was amplified and Gateway cloned into pDEST22 (Invitrogen).

pDBLeu-LMI2N or LMI2C bait constructs were co-transformed into yeast (PJ69-4A) with either pDEST22-LFY or pDEST alone. After transformation, cells were plated on –Trp –Leu/SD media. Double transformants were grown in –Trp –Leu/SD liquid media overnight, adjusted for equal cell density, serially diluted (10^{-1}-10^{-4}) and spotted on –Trp –Leu –His/SD plates.

Bimolecular fluorescence complementation

LMI2N and LMI2C fragments were inserted into pENTR3C (Invitrogen) and Gateway cloned into pCL113 (pBATL). The coding region of *LFY* was cloned into pCL112 (pBATL) to create the nYFP. p35S::2xmCherry was cloned into pEarley102 (Earley et al., 2006). The control protein (NC^b: TDY1-NLS in pCL113) was previously described (Ma et al., 2009). Constructs were transformed into onion epidermal cells using the PDS-1000/He Biolistic Particle Delivery System (BioRad, Hercules, CA, USA) as described by Ma et al. (Ma et al., 2009). Protein interactions were observed using an Olympus MVX10 fluorescent microscope.

RESULTS

LMI2 regulates the meristem identity transition

To elucidate the role of LMI2 in the meristem identity transition, we analyzed three T-DNA insertion alleles (Alonso and Stepanova, 2003): *lmi2-1*, *lmi2-2* and *lmi2-3* (Fig. 1A). In *lmi2-1*, the T-DNA insertion was located in the promoter region (116 bp from the transcription start site), whereas the insertions in *lmi2-2* and *lmi2-3* were located in the conserved MYB DNA binding domain (Fig. 1A). All three T-DNA insertions caused deletions in the *LMI2* locus ranging in size from 4 to 41 bp (Fig. 1A).

Both *lmi2-2* and *lmi2-3* expressed RNA upstream of the T-DNA insertion, suggesting that they are not RNA-null alleles (Fig. 1B). However, we did not detect *LMI2* expression in either the *lmi2-2* or the *lmi2-3* mutant using primers flanking the T-DNA insertions (Fig. 1B). Hence, these insertions probably give rise to a truncated non-functional LMI2 protein lacking part of the conserved DNA binding domain. The *lmi2-1* mutant, however, expressed elevated levels of *LMI2* RNA (Fig. 1B). As the T-DNA insertion in *lmi2-1* is located in the promoter region, it is likely that this insertion generates a full length *LMI2* transcript. Nonetheless, our combined data (see below) suggests that *lmi2-1* is a loss-of-function allele. Because *lmi2-2* and *lmi2-3* have similar T-DNA insertion sites, we chose to focus on the *lmi2-1* and *lmi2-2* alleles.

We assessed the timing of the meristem identity transition in *lmi2* mutants compared with wild type by counting the number of secondary inflorescences and cauline leaves formed prior to the formation of the first flower (Saddic et al., 2006; Yamaguchi et al., 2009). Flowering time was measured by counting the number of rosette leaves (see Table S1 in the supplementary material) (Yamaguchi et al., 2009). *lmi2-2* displayed a statistically significant increase in the number of cauline leaves and secondary inflorescences formed compared with wild type in five independent experiments (Table 1; Fig. 1C), suggesting that LMI2 plays a non-redundant role in the meristem identity transition. *lmi2-1* exhibited a more subtle delay in the meristem identity transition that differed significantly from wild type in only some of the experiments performed (Table 1; Fig. 1C).

All three *lmi2* alleles significantly enhanced the meristem identity phenotype of the weak *lfy-10* mutant in at least six independent experiments (Table 1; Fig. 1D,E). *lmi2-2 lfy-10* double mutants showed the strongest meristem identity delay, essentially phenocopying the *lfy-1* null mutant (Fig. 1E). In addition, in the *lfy-10* background, *lmi2-2*, and to a lesser extent *lmi2-1*, caused a delay in the meristem identity transition in heterozygotes (see Fig. S1 in the supplementary material). Hence, *LMI2* is a dosage-sensitive gene, at least under conditions when LFY activity is impaired. *LFY* itself is also dosage dependent (Blazquez et al., 1997; Okamuro et al., 1996), highlighting the sensitivity of this pathway to the level of both regulators. Finally, *lmi2-2* and *lmi2-1* displayed a subtle delay in flowering time (see Table S1 in the supplementary material) both as single mutants and in the *lfy-10* genetic background.

We next tested whether the mutations in *LMI2* caused the delay in the meristem identity transition by performing phenotypic rescue. Transformation of *lmi2-2 lfy-10* with a genomic copy of *LMI2* (pLMI2:LMI2) restored *LMI2* expression to a level similar to that observed in *lfy-10* (Fig. 1F). In addition, pLMI2:LMI2 fully rescued the enhanced meristem identity defects of *lmi2-2 lfy-10* relative to *lfy-10* (Fig. 1G).

To test whether LMI2 has additional LFY-independent roles during the meristem identity transition, we crossed the *lmi2-2* allele to the *lfy-1* null mutant. *lmi2-2* significantly enhanced the meristem identity transition defect of *lfy-1* (Table 1) indicating that LMI2 acts both downstream of and in parallel to LFY in this pathway. This is similar to AP1, which also acts downstream of and in parallel to LFY (Bowman et al., 1993).

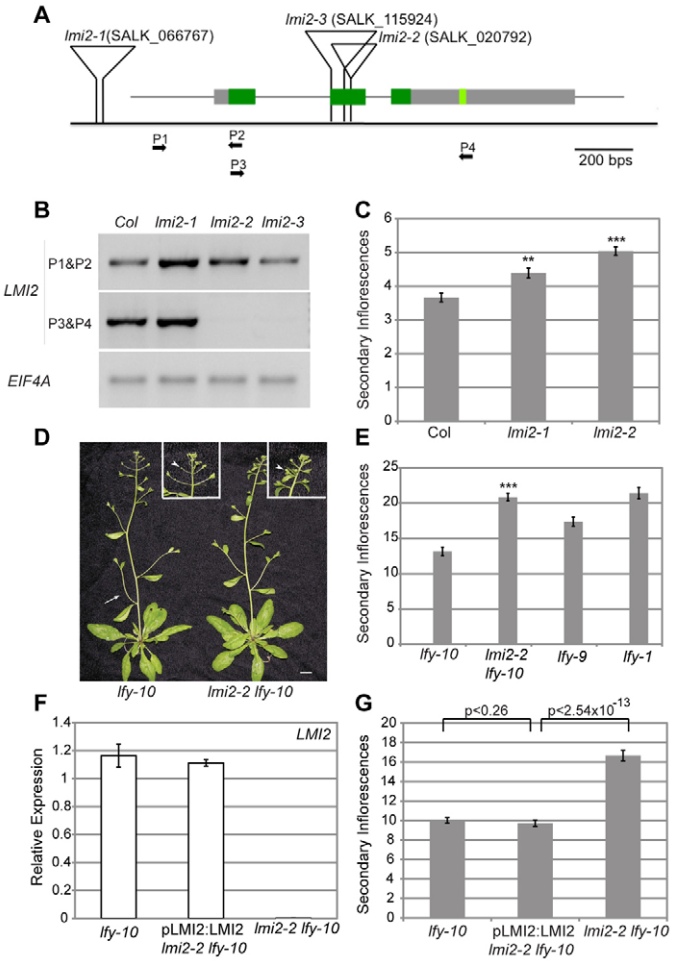

Fig. 1. *lmi2* mutants cause a meristem identity phenotype. (**A**) Map of the *LMI2* locus. Gray boxes, exons; gray line, 5′ and 3′ UTR and introns; dark green boxes, MYB DNA binding domain; light green box, conserved amino acid motif found in LMI2 and its homologs (Kranz et al., 1998; Stracke et al., 2001); triangles, T-DNA insertions. The lines connecting each T-DNA to the sequence denote the size of the deletion caused by each insertion. P1-P4, primers used for RT-PCR. (**B**) Semi-quantitative RT-PCR of *LMI2* expression performed on nine-day-old seedlings for each T-DNA insertion line and Col (wild type). Primers used (see A for location) are indicated at the left. The *EUKARYOTIC TRANSLATION INITIATION FACTOR 4A* (*EIF4A*) gene was used as an internal control. (**C**) Number of secondary inflorescences formed in *lmi2* single mutants compared with Col (wild type). (**D**) *lfy-10* and *lmi2-2 lfy-10* mutant phenotypes, with close-ups of the inflorescence apices (insets). Arrow indicates a secondary inflorescence subtended by a cauline leaf. Arrowheads indicate lateral organs formed in *lmi2-2 lfy-10* and *lfy-10* at a comparable stage. Scale bar: 1 cm. (**E**) Number of secondary inflorescences of *lmi2-2 lfy-10* compared with *lfy-10* (weak), *lfy-9* (intermediate) and *lfy-1* (strong) alleles. (**F**) qRT-PCR of *LMI2* expression in thirteen-day-old *lfy-10*, pLMI2:LMI2 *lmi2-2 lfy-10* and *lmi2-2 lfy-10* seedlings. (**G**) Number of secondary inflorescences formed in pLMI2:LMI2 *lmi2-2 lfy-10* compared with *lfy-10* and *lmi2-2 lfy-10*. $**P<10^{-3}$ (*lmi2-1* compared with Col); $***P<10^{-9}$ (*lmi2-2* and *lmi2-2 lfy-10* compared with Col and *lfy-10*, respectively); one-tailed Student's *t*-test. All values represent mean ± s.e.m.

Table 1. Meristem identity phenotypes of *lmi2* mutants

Genotype	Cauline leaves	Student's *t*-test	Secondary inflorescences	Student's *t*-test
Wild type (Col)	3.1±0.1 (33)		3.1±0.1 (33)	
lmi2-1	3.5±0.1 (32)	3/5	3.5±0.1 (32)	2/5
lmi2-2	4.1±0.1 (33)	5/5	4.1±0.1 (33)	5/5
lfy-10	6.0±0.1 (28)		11.4±0.4 (28)	
lmi2-1 lfy-10	11.5±0.5 (24)	6/6	15.7±0.5 (24)	6/6
lmi2-2 lfy-10	13.6±0.3 (28)	9/9	14.9±0.3 (28)	9/9
lfy-10	7.0±0.2 (37)		12.4±0.4 (37)	
lmi2-3 lfy-10	11.8±0.4 (14)	6/6	17.1±0.7 (14)	6/6
lfy-1	10.7±0.3 (21)		21.3±0.6 (21)	
lmi2-2 lfy-1	13.1±0.3 (17)	3/3	37.5±1.9 (17)	3/3

Average number of cauline leaves and secondary inflorescences ± s.e.m. for one representative experiment are shown. The number of plants counted is indicated in the parentheses. All phenotypic experiments were performed multiple times and one-sided Student's *t*-tests were performed for each experiment. The alternative hypothesis (H_1) is *lmi2* mutants have more lateral organs compared with the control genotype. Listed under Student's *t*-test are the number of experiments with a *P*-value less than 0.05 out of the total number of experiments performed.

LMI2 is expressed in the inflorescence meristem, in young floral primordia and in flowers

We first examined the expression of *LMI2* during the meristem identity transition using a bacterial β-glucuronidase (GUS) transcriptional reporter. In nine-day-old wild-type seedlings, *LMI2:GUS* was expressed in the center of the rosette close to the shoot apex (Fig. 2A) in a pattern roughly similar to that of *pLFY:GUS* (Fig. 2E). In the inflorescence, the *LMI2:GUS* reporter was expressed in the meristem proper and in young floral primordia, as well as in the carpels of older flowers (Fig. 2B-D; see Fig. S2A in the supplementary material). By contrast, as previously reported (Blazquez et al., 1997), *pLFY:GUS* expression was absent from the meristem proper but was observed in young floral primordia as well as in older flower primordia (Fig. 2F,G; see Fig. S2B in the supplementary material). In addition, both *LMI2:GUS* and *pLFY:GUS* were strongly expressed in secondary inflorescences (Fig. 2D,H). Thus, *LMI2:GUS* and *pLFY:GUS* have overlapping, but not identical, expression patterns during reproductive development.

LMI2:GUS expression was reduced in the shoot apex of intermediate *lfy-9* mutants compared with wild-type seedlings (see Fig. S2C,D in the supplementary material). Conversely, steroid treatment of an inducible version of LFY, LFY-GR (William et al., 2004), resulted in elevated *LMI2:GUS* expression in seedlings; this was not observed in steroid treated wild-type seedlings expressing *LMI2:GUS* (see Fig. S2E,F in the supplementary material). Therefore, LFY acts on *LMI2* cis regulatory elements present in this reporter construct, consistent with in vivo LFY binding to this locus (Winter et al., 2011).

We next examined endogenous *LMI2* expression by in situ hybridization. *LMI2* was expressed throughout the shoot apical meristem of primary inflorescences, with the highest expression observed in the young flower primordia (Fig. 2I). *LMI2* expression was reduced, but not absent, in the young flower primordia of *lfy-1* null mutant apices (Fig. 2J). No signal was observed using a sense probe (Fig. 2K). The residual *LMI2* expression in *lfy-1* is consistent with our genetic data that revealed an LFY-independent role for LMI2 in addition to its function downstream of LFY.

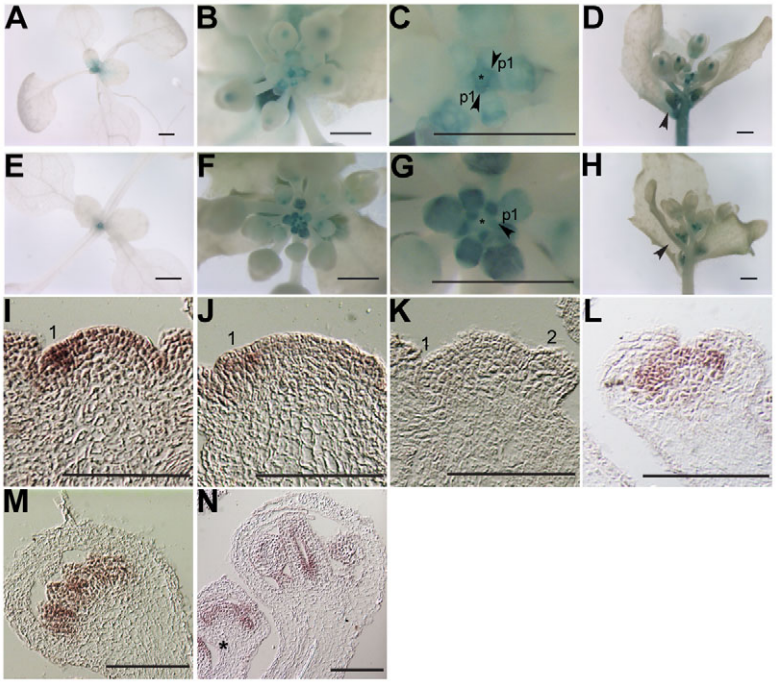

Fig. 2. *LMI2* is expressed in the initiating floral primordia and in developing flowers. (**A-H**) Expression of *LMI2:GUS* (A-D) and *pLFY:GUS* (E-H). Scale bars: 1 mm. (A,E) Nine-day-old seedlings. (B,F) Young (1 cm bolt) primary inflorescences. (C,G) Higher magnification of the shoot apices shown in B and F. Black arrowheads point to stage 1 floral primordia (p1) and asterisks indicate the shoot apical meristem. (D,H) *GUS* reporter expression in flowers and secondary inflorescences formed on 1 cm bolt primary inflorescences. Black arrowheads point to secondary inflorescences. (**I-N**) *LMI2* expression based on in situ hybridization. Scale bars: 100 μm. Numbers indicate the developmental stage of young floral primordia (Smyth et al., 1990). Expression in wild type (I,K-N) and *lfy-1* (J). Tissues assayed were: primary inflorescence apices (1 cm bolt; I-K), developing flowers at stage 4 (L), stage 7 (M) and stage 6 (asterisk), as well as stage 8 (N). Sense probe control is shown in K.

Subsequent to the meristem identity transition, *LMI2* was expressed in stage 2 to stage 4 flowers (Fig. 2L; data not shown) (Smyth et al., 1990) and in the developing stamens and carpels of older flowers from stage 6 to stage 8 (Fig. 2M,N). Eventually, in stage 8 flowers, *LMI2* expression decreased in the developing stamens but persisted in the carpels (Fig. 4N).

lmi2-1 acts as a loss-of-function allele

lmi2-1 displayed elevated *LMI2* expression in seedlings based on semi-quantitative RT-PCR (Fig. 1B), yet behaved as a loss-of-function allele (Table 1; Fig. 1C; see Fig. S1 in the supplementary material). Moreover, the defect in *lmi2-1 lfy-10* was rescued by pLMI2:LMI2 (Fig. 3A). In contrast to the wild type, *LMI2* expression was undetectable in *lmi2-1* shoot apices and young flower primordia (Fig. 3B,C), similar to the sense control (Fig. 3D). Thus, in *lmi2-1* mutants, *LMI2* is absent from the initiating floral primordia, where it is required for the meristem identity transition. This suggests that the increased *LMI2* levels observed by RT-PCR could be due to ectopic *LMI2* expression. Indeed, whereas *LMI2* expression was very low in the roots and leaves of nine-day-old wild-type seedlings, it was strongly expressed in these tissues in *lmi2-1* (a 40-fold and 400-fold increase, respectively; Fig. 3E). Based on our combined findings, we conclude that the T-DNA insertion in *lmi2-1* apparently disrupts the *LMI2* promoter, causing loss of *LMI2* expression in the shoot apical meristem and in the young flower primordia. At the same time, the insertion causes ectopic and elevated *LMI2* expression, perhaps from a promoter located in the T-DNA insertion.

LMI2 is required for proper *AP1* upregulation

To place LMI2 in the meristem identity pathway, we examined the expression of the direct LFY targets *AP1*, *CAL*, *LMI1* to *LMI5*, and that of another meristem identity regulator, *FRUITFULL* (*FUL*) (Ferrandiz et al., 2000; Wagner et al., 1999; William et al., 2004) in *lfy-10* single mutants compared with *lmi2-2 lfy-10* double mutants during the meristem identity transition (Fig. 4A, see Fig. S3A in the supplementary material). We conducted a time-course experiment spanning time points prior to, during and immediately subsequent to the meristem identity transition for all genotypes tested (Fig. 4A,B-E) (William et al., 2004; Yamaguchi et al., 2009). Although we did not observe a reduction in the expression of *LMI1*, *LMI3* or *LMI5*, we observed a subtle reduction in the expression of *LMI4* and a pronounced (approximately fourfold) reduction in the expression of *AP1* in *lmi2-2 lfy-10* compared with *lfy-10* at day 13 (Fig. 4A; see Fig. S3A in the supplementary material). Indeed, *AP1* expression was induced more slowly in the double mutant compared with *lfy-10* (Fig. 4A). By contrast, induction of *CAL* and *FUL* expression was very similar in *lfy-10* and *lmi2-2 lfy-10* plants, suggesting that the observed defect in *AP1* upregulation is specific. *AP1* expression was also reduced in *lmi2-2/+ lfy-10* plants relative to *lfy-10* mutants (see Fig. S3B in the supplementary material), consistent with the observed dosage sensitivity of *LMI2*, as well as in *lmi2-2* single mutant seedlings compared with wild type (Fig. 4G). Our combined data suggest that LMI2 acts upstream of *AP1*.

lfy null mutants cause a delay, but not a loss in *AP1* expression; *AP1* is expressed in the flowers that eventually form in these mutants (Ruiz-Garcia et al., 1997; Wagner et al., 1999). Likewise, based on qRT-PCR, *AP1* is upregulated in *lmi2-2 lfy-10*, reaching expression levels similar to those observed in *lfy-10* at day 15 (Fig. 4A), when flower patterning is initiated (see Fig. S3C in the supplementary material).

We next examined *AP1* upregulation in wild-type, *lfy-10* and *lmi2-2 lfy-10* seedlings using in situ hybridization. By day 13, all three genotypes had initiated the first flowers. *AP1* expression was much reduced in stage 1 or 2 flower primordia in thirteen-day-old *lmi2-2 lfy-10* and the *lfy-10* mutants relative to wild type (Fig. 4B-E; data not shown). In addition, *AP1* expression levels were slightly more reduced in developing flower primordia of *lmi2-2 lfy-10* compared with *lfy-10* (Fig. 4C-E), and in the double mutants especially in the shoot meristem proximal region of stage 2 flower primordia (Fig. 4D,E).

To test whether LMI2 can regulate *AP1* expression directly, we scanned the *AP1* locus for the presence of plant MYB binding sites using AthaMap (http://www.athamap.de/) (Steffens et al., 2004). Eight predicted MYB binding sites were found in the 5′ upstream region; two in the introns and one in the first exon of *AP1* (Fig. 4F). We next examined whether LMI2 binds to *AP1* regulatory regions in vivo by anti-HA chromatin immunoprecipitation (ChIP) followed by qPCR using plants expressing a HA-tagged genomic version of *LMI2* driven from its own promoter (pLMI2:LMI2-HA). The LMI2-HA fusion protein is biologically active, as pLMI2:LMI2-HA *lmi2-2* rescued the reduced *AP1* expression observed in *lmi2-2* mutants (Fig. 4G). LMI2-HA was recruited to the *AP1* promoter and bound to region six of *AP1*, which is very close to the known or predicted binding sites of other regulators of *AP1*, including LFY (Fig. 4F,H) (Abe et al., 2005; Parcy et al., 1998; Wang et al., 2009; Wigge et al., 2005; William et al., 2004; Winter et al., 2011; Xu et al., 2010; Yamaguchi et al., 2009). By contrast, we did not see enrichment of LMI2-HA relative to control *lmi2-2* plants in the remaining regions of the *AP1* locus, suggesting that the binding of LMI2 at region six is specific (Fig. 4H). Taken together, our data suggest that LMI2 directly activates *AP1* expression during the meristem identity transition.

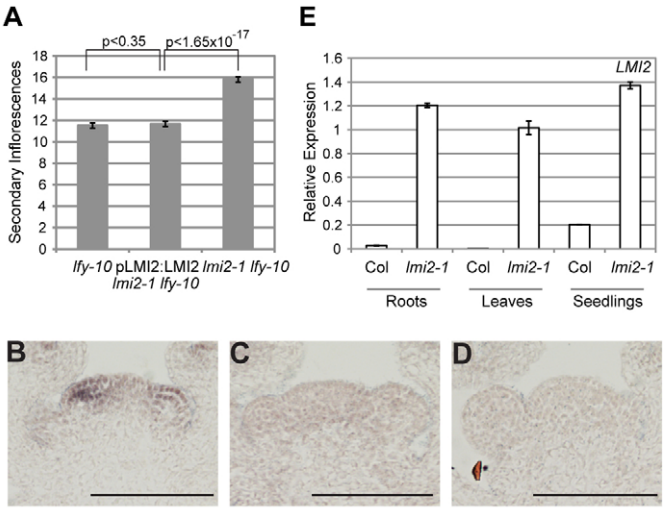

Fig. 3. The T-DNA insertion in *lmi2-1* causes misregulation of *LMI2*. (**A**) The number of secondary inflorescences in pLMI2:LMI2 *lmi2-1 lfy-10* compared with *lfy-10* and *lmi2-1 lfy-10*. *P*-values for one-tailed Student's *t*-test are indicated. (**B**,**C**) *LMI2* expression based on in situ hybridization in wild-type (B) and *lmi2-1* (C) 1 cm bolt primary inflorescences. (**D**) *LMI2* sense probe control. Scale bars: 100 μm. (**E**) qRT-PCR analysis of *LMI2* expression in roots (including hypocotyl), leaves (including cotyledons) and whole seedlings from nine-day-old wild type (Col) and *lmi2-1* mutants. Values are mean ± s.e.m.

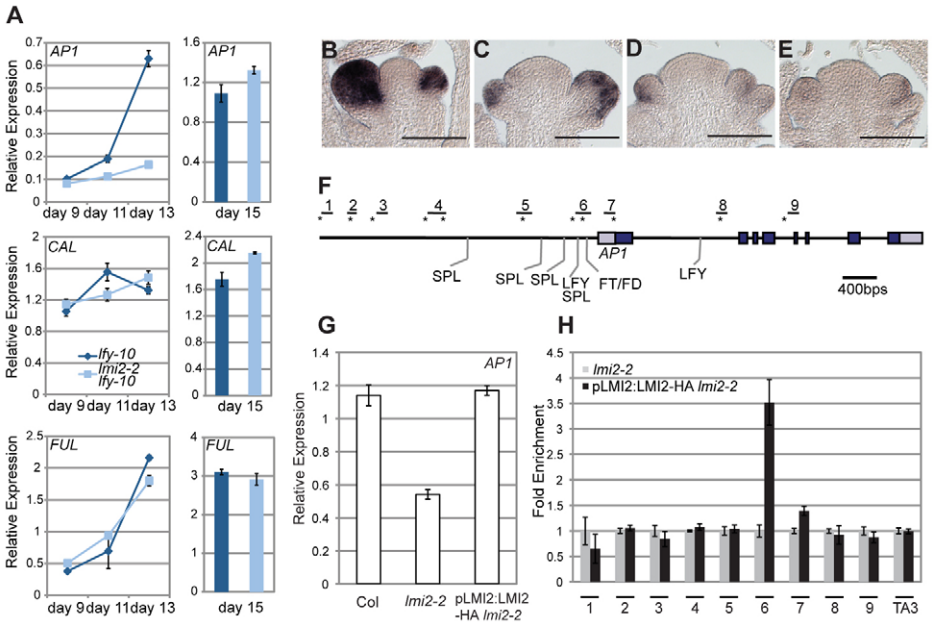

Fig. 4. LMI2 is required for proper activation of *AP1* expression. (**A**) *AP1*, *CAL* and *FUL* expression in *lfy-10* and *lmi2-2 lfy-10* seedlings based on qRT-PCR at days 9, 11, 13 and 15. Values represent mean ± s.e.m. (**B-E**) *AP1* expression based on in situ hybridization of eleven-day-old wild-type (Col; B) and thirteen-day-old *lfy-10* (C) and *lmi2-2 lfy-10* (D,E) seedlings. Scale bars: 100 μm. (**F**) Map of the *AP1* locus. Light purple boxes, 5′ and 3′ UTRs; dark purple boxes, exons; black lines, introns and intergenic regions; asterisks, predicted plant MYB binding sites with a score exceeding the threshold score (Steffens et al., 2004); horizontal bars, regions amplified in ChIP q-PCR. Binding sites of known regulators of *AP1* are shown below the locus (see text for details). (**G**) Rescue of *AP1* expression in eleven-day-old pLMI2:LMI2-HA *lmi2-2* seedlings. (**H**) ChIP-qPCR in eleven-day-old *lmi2-2* and pLMI2:LMI2-HA *lmi2-2* seedlings to assess LMI2 binding to *AP1* regulatory regions. Immunoprecipitated DNA is represented as fold enrichment relative to the *lmi2-2* control. Values shown are mean ± s.e.m. The heterochromatic *TA3* retrotransposon (Konieczny et al., 1991) served as a negative ChIP control.

To test whether LMI2 acts solely to induce *AP1* or whether it regulates other factors during the meristem identity transition, we crossed *lmi2-2* to the strong *ap1-10* mutant and examined the timing of the meristem identity transition. We did not observe an increase in the number of secondary inflorescences in *lmi2-2 ap1-10* compared with *ap1-10*. There was, however, a significant increase in the number of cauline leaves produced in *lmi2-2 ap1-10* compared with *ap1-10* (Table 2). AP1 does not play a significant role in cauline leaf suppression during the floral transition (Bowman et al., 1993; Schultz and Haughn, 1993). Thus, like LFY (Liljegren et al., 1999), LMI2 functions through an AP1-independent pathway to suppress cauline leaf formation. We conclude that LMI2 acts both upstream of and in parallel to AP1 during the meristem identity transition.

Interactions between LMI2 and LFY

LMI2 binds very close to the known LFY binding site in the *AP1* locus (one putative LMI2 binding site in region six is 6 bp downstream of the LFY binding site; data not shown) (Winter et al., 2011). Hence, LMI2 and LFY might interact physically. Indeed, based on pull-down assays, LMI2 interacted with GST-LFY (Fig. 5A). Full length LFY protein homodimerized, as previously proposed (Hames et al., 2008), serving as a positive control. A negative control protein (see Materials and methods for details) did not interact with GST-LFY, confirming the specificity of the observed interactions (Fig. 5A).

Based on yeast two-hybrid assays, the N-terminal half of LMI2 (LMI2N) showed a weak, but reproducible interaction with LFY (Fig. 5B). The C-terminal domain of LMI2 (LMI2C) also interacted with LFY in yeast (data not shown). This interaction was more difficult to observe because, as previously reported (Zhang et al., 2009), this domain of LMI2 displays transcriptional activation activity. Finally, bimolecular fluorescence complementation (BiFC) was used to test for an in vivo interaction between LMI2 and LFY. Both the LMI2N and, to a lesser extent, LMI2C interacted with LFY (Fig. 5C). Again, LFY interacted with itself. By contrast, a negative control protein did not interact with LFY, suggesting the observed interactions were specific. The combined data suggest that LFY and LMI2 can form heterodimers.

During the floral transition, LFY and AP1 act in a positive feedback regulatory loop (Ferrandiz et al., 2000; Kaufmann et al., 2010; Liljegren et al., 1999). In light of this, we examined whether

Table 2. Meristem identity phenotypes of *lmi2 ap1* mutants

Genotype	Cauline leaves	Student's *t*-test	Secondary inflorescences	Student's *t*-test
ap1-10	3.6±0.2 (12)		3.8±0.3 (12)	
lmi2-2 ap1-10	4.2±0.2 (13)	4/5	4.0±0.2 (13)	0/5

Average number of cauline leaves and secondary inflorescences ± s.e.m. for one representative experiment are shown. The number of plants counted is indicated in parentheses. All phenotypic experiments were performed multiple times and one-sided Student's *t*-tests were performed for each experiment. The alternative hypothesis (H_1) is *lmi2* mutants have more lateral organs compared with the control genotype. Listed under Student's *t*-test are the number of experiments with a *P*-value less than 0.05 out of the total number of experiments performed.

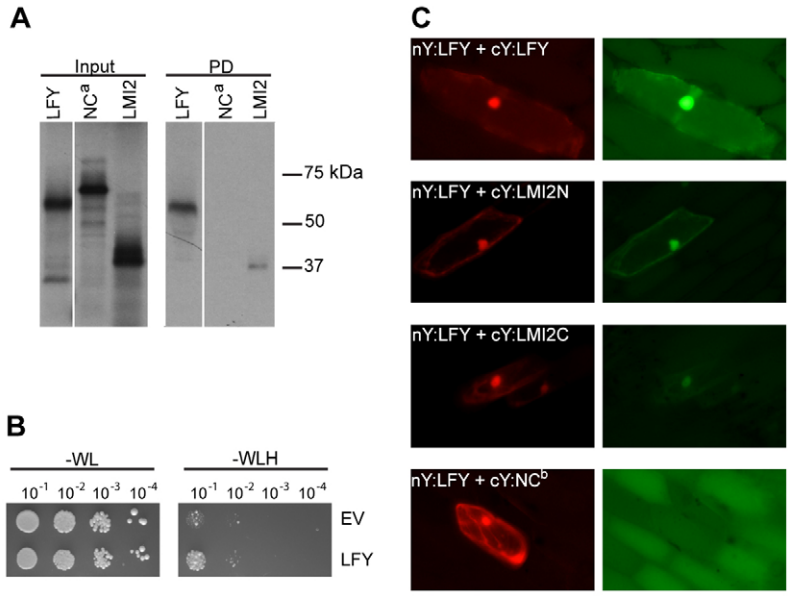

Fig. 5. LMI2 interacts physically with LFY. (**A**) In vitro GST-pull-down assay. GST-tagged LFY protein incubated with in vitro translated LFY, LMI2 and a negative control peptide (NC^a). 5% input is shown. Input and pull-down (PD) were run on the same gel, spaces between lanes denote irrelevant samples removed from the gel image. Molecular weight markers (kDa) are indicated on the right. (**B**) Yeast two-hybrid assay. Growth of yeast transformed with pDBLeu-LMI2N bait construct and pDEST22-LFY or pDEST22 alone (EV) on –Trp –Leu/SD plates (–WL) or –Trp –Leu –His/SD plates (–WLH). (**C**) Interaction of LMI2N and LMI2C with LFY based on bimolecular fluorescence complementation (BiFC). Left: 35S:2XmCherry transformation control. Right: protein interactions. Positive control: nY:LFY and cY:LFY. Negative control: nY:LFY and $cY:NC^b$.

LMI2 can also feedback to regulate *LFY*. Indeed, *LFY* levels were reduced in *lmi2-2 lfy-10* compared with *lfy-10* mutants throughout the meristem identity transition (Fig. 6A). Furthermore, *LFY* levels were reduced in eleven-day-old *lmi2-2* seedlings compared with wild type (Col) (Fig. 6B). To determine whether the reduction in *LFY* in *lmi2* mutants was an indirect consequence of reduced *AP1* expression in these mutants or whether LMI2 directly regulated *LFY* levels, we used ChIP to examine LMI2 binding to *LFY* regulatory regions. We tested binding of LMI2 to three predicted MYB binding sites in the 5′ upstream regulatory region: two sites in exon one and two sites in the second intron of *LFY* (Fig. 6C). We did not see binding of LMI2-HA to the promoter or intron regions of *LFY*, but we did observe a subtle enrichment at region four in exon one (Fig. 6D). Although one other LFY regulator has previously been shown to bind this region (Yamaguchi et al., 2009), further experiments are needed to determine whether the feedback from LMI2 to *LFY* is direct.

DISCUSSION

LMI2 is a meristem identity regulator downstream of LFY

We show here that the direct LFY target and MYB transcription factor LMI2 is required for correct timing of the meristem identity transition in *Arabidopsis*. *LMI2* was identified by two independent genomic approaches as a direct LFY-regulated and LFY-bound target during meristem identity transition (William et al., 2004; Winter et al., 2011). Notably, unlike two other known meristem identity regulator mutants (*cal* and *lmi1*) (Bowman et al., 1993; Saddic et al., 2006), *lmi2* single mutants displayed a statistically significant delay in the meristem identity transition, suggesting a central role for this transcription factor in the timing of flower formation. Thus far, only one other direct LFY target has a non-redundant role in this vital developmental transition: *AP1* (Bowman et al., 1993; Weigel et al., 1992).

Additional roles for LMI2 at other stages of reproductive development

The observed *LMI2* expression pattern suggests that LMI2 might have a broad role in reproductive development. Like many flowering-time regulators (Abe et al., 2005; Hempel et al., 1997; Lee et al., 2000; Wigge et al., 2005), *LMI2* was expressed in the shoot apex, and LMI2 controls the timing of bolting. In addition, both *LFY* and *LMI2* were expressed in older flower primordia. Unlike *lfy* mutants (Huala and Sussex, 1992; Weigel et al., 1992), *lmi2* mutants did not display noticeable floral homeotic defects nor did they enhance the floral homeotic defects of weak *lfy* mutants (data not shown), suggesting that LMI2 might have a different role in flower development.

LMI2 directly activates *AP1* to promote floral fate

AP1 upregulation signals commitment to flower formation and, therefore, must be tightly controlled for proper timing of the meristem identity transition (Bowman et al., 1993; Kaufmann et al., 2010; Mandel et al., 1992; Wellmer and Riechmann, 2010). Here, we provide evidence that LMI2 directly upregulates *AP1* expression during the meristem identity transition. The effect of LMI2 on *AP1* expression is specific and is not due to a general delay in phase transitions, because accumulation of other meristem identity regulators, such as *FUL* or *CAL* (Bowman et al., 1993; Ferrandiz et al., 2000), are not altered in *lmi2-2 lfy-10* mutants. *LMI2* induction precedes that of *AP1* and both are expressed in stage 1 floral primordia, where AP1 directs flower development (this study) (Liljegren et al., 1999; Mandel et al., 1992; Schmid et al., 2005). LMI2 binds to a region of the *AP1* locus also occupied by many other transcription factors in vivo, including LFY (Wang et al., 2009; William et al., 2004; Xu et al., 2010; Yamaguchi et al., 2009), thus defining a critical *AP1* cis regulatory module (Jeziorska et al., 2009; Wilczynski and Furlong, 2010).

LMI2 and LFY interact physically

The LMI2 and LFY binding sites on the *AP1* promoter are very close to each other and, based on three independent assays, the LMI2 and LFY proteins interact physically. MYB proteins are known to interact with other transcription factors to regulate gene expression (Li et al., 2009; Shin et al., 2007; Zimmermann et al., 2004). LFY also interacts with cofactors, including at least one other downstream target, to regulate gene expression (Chae et al., 2008; Lenhard et al., 2001; Liu et al., 2009b; Lohmann et al., 2001; Winter et al., 2011). For example, LFY directly

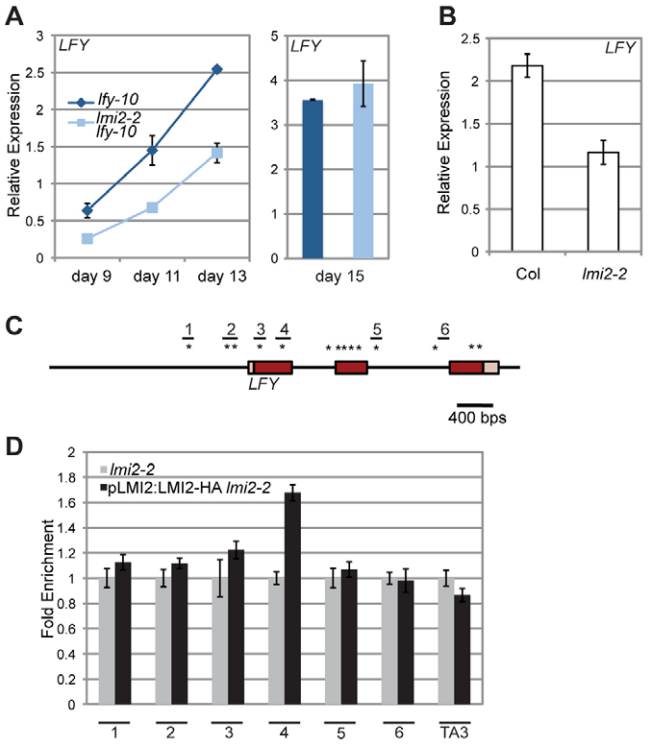

Fig. 6. LMI2 regulates *LFY* expression by positive feedback during the floral transition. (**A**) *LFY* expression based on qRT-PCR in *lfy-10* and *lmi2-2 lfy-10* seedlings at days 9, 11, 13 and 15. (**B**) *LFY* expression in eleven-day-old wild-type (Col) and *lmi2-2* seedlings. (**C**) *LFY* Locus. Light red boxes, 5′ and 3′ UTRs; dark red boxes, exons; black lines, introns and intergenic regions; asterisks, predicted plant MYB binding sites (see Fig. 4F). (**D**) ChIP q-PCR to test for LMI2-HA binding to *LFY* regulatory loci. See Fig. 4H for details on the ChIP analysis. Values shown are mean ± s.e.m.

upregulates the floral homeotic regulator *SEPALLATA3* (*SEP3*) and, in turn, these two factors interact physically to activate the class B and C floral homeotic genes (Liu et al., 2009b; Winter et al., 2011).

Based on the recent finding that LFY acts as both a direct transcriptional activator and repressor (Parcy et al., 2002; William et al., 2004; Winter et al., 2011), it seems likely that cofactors modulate the effect of LFY on gene expression. Consistent with this idea, LFY alone is unable to activate gene expression from the *AP1* promoter in yeast: it can only act as a transcriptional activator in this system when fused to a strong activation domain (Parcy et al., 1998; Winter, 2011). It is likely that LFY also needs a co-activator for *AP1* induction in vivo. LMI2 is a good candidate for this LFY co-activator: it has strong transactivation activity based on yeast assays, it is induced by LFY prior to *AP1* upregulation and can form heterodimers with LFY (this study) (Blazquez et al., 1997; Hempel et al., 1997; Schmid et al., 2005; Schmid et al., 2003; Zhang et al., 2009). Moreover, the temporal delay in the formation of the first flower is very similar in *ap1* and *lmi2* single mutants (this study) (Xu et al., 2010); thus, LMI2 might be sufficient for LFY-dependent activation of *AP1* expression. However, we cannot rule out that other LFY co-factors contribute to this process.

The LFY, LMI2 and AP1 regulatory network might contribute to an abrupt and robust meristem identity transition

The observed interactions between LFY, LMI2 and AP1 represent a coherent feed-forward loop (Fig. 7) (Alon, 2007), a regulatory circuit with crucial roles in control of developmental processes in many organisms (Alon, 2007; Mangan et al., 2003; Shen-Orr et al., 2002). The type of coherent feed-forward loop observed here serves as a persistence detector for inductive signal(s) and as a temporal delay element (Alon, 2007). Thus, transient inductive cues that cause a temporary increase in *LFY*, but not in *LMI2*, will delay LFY-dependent upregulation of *AP1*.

This finding is consistent with prior observations. For example, *LFY* upregulation is directed by environmental cues, such as changes in day length or ambient temperature (Amasino, 2010; Kobayashi and Weigel, 2007; Liu et al., 2009a); these stimuli are inherently noisy inputs, yet the transition to flower formation is abrupt in *Arabidopsis*, without formation of intermediate structures (Parcy, 2005). In addition, as discussed above, *AP1* induction is delayed with respect to that of *LFY* and *LMI2*, and is reduced in both single mutants. Finally, as predicted by the feed-forward loop model, *LMI2* was a haplo-insufficient, rate-limiting factor for *AP1* induction downstream of LFY, at least under conditions when LFY activity was compromised.

In addition to the feed-forward loop uncovered here, LFY directs at least two additional coherent feed-forward loops, one of which is also linked to the meristem identity transition and involves the direct LFY targets *LMI1* and *CAL* (Fig. 7) (Kaufmann et al., 2009; Liu et al., 2009b; Saddic et al., 2006; William et al., 2004; Winter et al., 2011). Among these feed-forward loops involving LFY, the LFY-LMI2-AP1 feed-forward loop stands out as it alone comprises three regulators that have non-redundant roles in the process they regulate; hence, it might represent a crucial regulatory module in the meristem identity transition.

In *Arabidopsis*, the meristem identity transition is not only precise (it occurs after formation of a defined number of secondary inflorescences subtended by cauline leaves), but also robust (no reversion from flower to inflorescence fate is observed) (Amasino, 2010; Blazquez et al., 2006; Liu et al., 2009a; Tooke et al., 2005). As outlined above, the LFY-LMI2-AP1 feed-forward loop is likely to contribute to the precision of this developmental transition; its robustness, however, might be

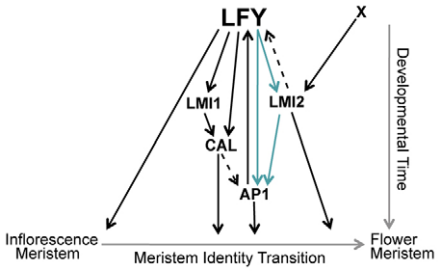

Fig. 7. Meristem identity pathway downstream of LFY. The LFY transcription factor directly activates multiple downstream factors during the meristem identity transition, including *CAL*, *LMI1*, *AP1* and *LMI2* (Saddic et al., 2006; William et al., 2004). *LMI2* is also upregulated by another factor, 'X', in a pathway parallel to LFY. LFY, LMI2 and AP1 act in a feed-forward loop (blue arrows) to initiate the meristem identity transition, and LMI2 and AP1 positively feedback to *LFY* (this study) (Kaufmann et al., 2010). Interactions, which could be indirect or direct, are indicated by dashed arrows.

due to positive feedback (Alon, 2007). Indeed, a positive direct feedback from AP1 to *LFY* has recently been described (Kaufmann et al., 2010; Liljegren et al., 1999). We show here that LMI2 also positively regulates *LFY*: *LFY* expression was reduced in *lmi2-2* single and double mutants. This reduction of *LFY* expression could be an indirect effect, triggered by the reduced *AP1* expression levels observed in *lmi2-2* mutants. However, the positive feedback might, in part, be direct as LMI2 was weakly recruited to the *LFY* locus. The observed enhancement of the *ap1* mutant meristem identity defect by *lmi2* is consistent with this hypothesis. It is likely that the AP1 and possible LMI2 feedback loops keep the LFY-LMI2-AP1 feed-forward loop active after full *AP1* upregulation has been achieved. Indeed, AP1 directly downregulates upstream activators of itself and of LFY (Kaufmann et al., 2010), providing further support for the idea that the combined feed-forward and feedback loop is self-maintained.

It will be of interest to examine these regulatory interactions in other flowering plant species. In light of this question, we note that *LMI2* separated from its closest homologs, the *MIXTA*/*MYB16* and *MYB106* genes, before the split of the monocots from the eudicots ~100 million years ago (Baumann et al., 2007). This raises the possibility that the function of LMI2 in reproductive development evolved early in the flowering plant lineage and might be conserved in other angiosperm species.

Acknowledgements
We are grateful to David M. Braun for the BiFC negative control protein and to Jennifer Pfluger for the yeast two-hybrid and BiFC LFY constructs. We thank Kim Gallagher, John Wagner, Matthew Willmann and Cara M. Winter for critical comments and suggestions on this manuscript. This research was funded by NSF grant IOS 0849298 to D.W. and a NIH Training Grant 5-T32-HD007516 (Developmental Biology) as well as a University of Pennsylvania, School of Arts and Sciences, Dissertation Research Fellowship to J.J.P. Deposited in PMC for release after 12 months.

Competing interests statement
The authors declare no competing financial interests.

Supplementary material
Supplementary material for this article is available at
http://dev.biologists.org/lookup/suppl/doi:10.1242/dev.063073/-/DC1

References

Abe, M., Kobayashi, Y., Yamamoto, S., Daimon, Y., Yamaguchi, A., Ikeda, Y., Ichinoki, H., Notaguchi, M., Goto, K. and Araki, T. (2005). FD, a bZIP protein mediating signals from the floral pathway integrator FT at the shoot apex. *Science* **309**, 1052-1056.
Alon, U. (2007). Network motifs: theory and experimental approaches. *Nat. Rev. Genet.* **8**, 450-461.
Alonso, J. M. and Stepanova, A. N. (2003). T-DNA mutagenesis in Arabidopsis. *Methods Mol. Biol.* **236**, 177-188.
Amasino, R. (2010). Seasonal and developmental timing of flowering. *Plant J.* **61**, 1001-1013.
Araki, T. (2001). Transition from vegetative to reproductive phase. *Curr. Opin. Plant Biol.* **4**, 63-68.
Baumann, K., Perez-Rodriguez, M., Bradley, D., Venail, J., Bailey, P., Jin, H., Koes, R., Roberts, K. and Martin, C. (2007). Control of cell and petal morphogenesis by R2R3 MYB transcription factors. *Development* **134**, 1691-1701.
Baurle, I. and Dean, C. (2006). The timing of developmental transitions in plants. *Cell* **125**, 655-664.
Blazquez, M. A., Soowal, L. N., Lee, I. and Weigel, D. (1997). LEAFY expression and flower initiation in Arabidopsis. *Development* **124**, 3835-3844.
Blazquez, M. A., Ferrandiz, C., Madueno, F. and Parcy, F. (2006). How floral meristems are built. *Plant Mol. Biol.* **60**, 855-870.
Bowman, J. L., Alvarez, J., Weigel, D., Meyerowitz, E. M. and Smyth, D. R. (1993). Control of flower development In Arabidopsis thaliana By Apetala1 and interacting genes. *Development* **119**, 721-743.
Chae, E., Tan, Q. K., Hill, T. A. and Irish, V. F. (2008). An Arabidopsis F-box protein acts as a transcriptional co-factor to regulate floral development. *Development* **135**, 1235-1245.
Dubos, C., Stracke, R., Grotewold, E., Weisshaar, B., Martin, C. and Lepiniec, L. (2010). MYB transcription factors in Arabidopsis. *Trends Plant Sci.* **15**, 573-581.
Earley, K. W., Haag, J. R., Pontes, O., Opper, K., Juehne, T., Song, K. and Pikaard, C. S. (2006). Gateway-compatible vectors for plant functional genomics and proteomics. *Plant J.* **45**, 616-629.
Ferrandiz, C., Gu, Q., Martienssen, R. and Yanofsky, M. F. (2000). Redundant regulation of meristem identity and plant architecture by FRUITFULL, APETALA1 and CAULIFLOWER. *Development* **127**, 725-734.
Hames, C., Ptchelkine, D., Grimm, C., Thevenon, E., Moyroud, E., Gerard, F., Martiel, J. L., Benlloch, R., Parcy, F. and Muller, C. W. (2008). Structural basis for LEAFY floral switch function and similarity with helix-turn-helix proteins. *EMBO J.* **27**, 2628-2637.
Hempel, F. D., Weigel, D., Mandel, M. A., Ditta, G., Zambryski, P. C., Feldman, L. J. and Yanofsky, M. F. (1997). Floral determination and expression of floral regulatory genes in Arabidopsis. *Development* **124**, 3845-3853.
Huala, E. and Sussex, I. M. (1992). *LEAFY* interacts with floral homeotic genes to regulate Arabidopsis floral development. *Plant Cell* **4**, 901-913.
Jakoby, M. J., Falkenhan, D., Mader, M. T., Brininstool, G., Wischnitzki, E., Platz, N., Hudson, A., Hulskamp, M., Larkin, J. and Schnittger, A. (2008). Transcriptional profiling of mature Arabidopsis trichomes reveals that NOECK encodes the MIXTA-like transcriptional regulator MYB106. *Plant Physiol.* **148**, 1583-1602.
Jeziorska, D. M., Jordan, K. W. and Vance, K. W. (2009). A systems biology approach to understanding cis-regulatory module function. *Semin. Cell Dev. Biol.* **20**, 856-862.
Kaufmann, K., Muino, J. M., Jauregui, R., Airoldi, C. A., Smaczniak, C., Krajewski, P. and Angenent, G. C. (2009). Target genes of the MADS transcription factor SEPALLATA3: integration of developmental and hormonal pathways in the Arabidopsis flower. *PLoS Biol.* **7**, e1000090.
Kaufmann, K., Wellmer, F., Muino, J. M., Ferrier, T., Wuest, S. E., Kumar, V., Serrano-Mislata, A., Madueno, F., Krajewski, P., Meyerowitz, E. M. et al. (2010). Orchestration of floral initiation by APETALA1. *Science* **328**, 85-89.
Kobayashi, Y. and Weigel, D. (2007). Move on up, it's time for change mobile signals controlling photoperiod-dependent flowering. *Genes Dev.* **21**, 2371-2384.
Komeda, Y. (2004). Genetic regulation of time to flower in Arabidopsis thaliana. *Annu. Rev. Plant Biol.* **55**, 521-535.
Konieczny, A., Voytas, D. F., Cummings, M. P. and Ausubel, F. M. (1991). A superfamily of Arabidopsis thaliana retrotransposons. *Genetics* **127**, 801-809.
Koornneef, M., Alonso-Blanco, C., Peeters, A. J. and Soppe, W. (1998). Genetic control of flowering time in Arabidopsis. *Annu. Rev. Plant Physiol. Plant Mol. Biol.* **49**, 345-370.
Kranz, H. D., Denekamp, M., Greco, R., Jin, H., Leyva, A., Meissner, R. C., Petroni, K., Urzainqui, A., Bevan, M., Martin, C. et al. (1998). Towards functional characterisation of the members of the R2R3-MYB gene family from Arabidopsis thaliana. *Plant J.* **16**, 263-276.
Kwon, C. S., Chen, C. and Wagner, D. (2005). WUSCHEL is a primary target for transcriptional regulation by SPLAYED in dynamic control of stem cell fate in Arabidopsis. *Genes Dev.* **19**, 992-1003.
Lee, H., Suh, S. S., Park, E., Cho, E., Ahn, J. H., Kim, S. G., Lee, J. S., Kwon, Y. M. and Lee, I. (2000). The AGAMOUS-LIKE 20 MADS domain protein integrates floral inductive pathways in Arabidopsis. *Genes Dev.* **14**, 2366-2376.
Lenhard, M., Bohnert, A., Jurgens, G. and Laux, T. (2001). Termination of stem cell maintenance in Arabidopsis floral meristems by interactions between WUSCHEL and AGAMOUS. *Cell* **105**, 805-814.
Li, L., Yu, X., Thompson, A., Guo, M., Yoshida, S., Asami, T., Chory, J. and Yin, Y. (2009). Arabidopsis MYB30 is a direct target of BES1 and cooperates with BES1 to regulate brassinosteroid-induced gene expression. *Plant J.* **58**, 275-286.
Liljegren, S. J., Gustafson-Brown, C., Pinyopich, A., Ditta, G. S. and Yanofsky, M. F. (1999). Interactions among APETALA1, LEAFY, and TERMINAL FLOWER1 specify meristem fate. *Plant Cell* **11**, 1007-1018.
Liu, C., Zhou, J., Bracha-Drori, K., Yalovsky, S., Ito, T. and Yu, H. (2007). Specification of Arabidopsis floral meristem identity by repression of flowering time genes. *Development* **134**, 1901-1910.
Liu, C., Thong, Z. and Yu, H. (2009a). Coming into bloom: the specification of floral meristems. *Development* **136**, 3379-3391.
Liu, C., Xi, W., Shen, L., Tan, C. and Yu, H. (2009b). Regulation of floral patterning by flowering time genes. *Dev. Cell* **16**, 711-722.
Lohmann, J. U., Hong, R. L., Hobe, M., Busch, M. A., Parcy, F., Simon, R. and Weigel, D. (2001). A molecular link between stem cell regulation and floral patterning in Arabidopsis. *Cell* **105**, 793-803.
Long, J. A. and Barton, M. K. (1998). The development of apical embryonic pattern in Arabidopsis. *Development* **125**, 3027-3035.
Ma, Y., Slewinski, T. L., Baker, R. F. and Braun, D. M. (2009). Tie-dyed1 encodes a novel, phloem-expressed transmembrane protein that functions in carbohydrate partitioning. *Plant Physiol.* **149**, 181-194.
Mandel, M. A. and Yanofsky, M. F. (1995). A gene triggering flower formation in Arabidopsis. *Nature* **377**, 522-524.

Mandel, M. A., Gustafson-Brown, C., Savidge, B. and Yanofsky, M. F. (1992). Molecular characterization of the Arabidopsis floral homeotic gene APETALA1. *Nature* **360**, 273-277.
Mangan, S., Zaslaver, A. and Alon, U. (2003). The coherent feedforward loop serves as a sign-sensitive delay element in transcription networks. *J. Mol. Biol.* **334**, 197-204.
Martin, C. and Paz-Ares, J. (1997). MYB transcription factors in plants. *Trends Genet.* **13**, 67-73.
Nakagawa, T., Kurose, T., Hino, T., Tanaka, K., Kawamukai, M., Niwa, Y., Toyooka, K., Matsuoka, K., Jinbo, T. and Kimura, T. (2007). Development of series of gateway binary vectors, pGWBs, for realizing efficient construction of fusion genes for plant transformation. *J. Biosci. Bioeng.* **104**, 34-41.
Oh, E., Kang, H., Yamaguchi, S., Park, J., Lee, D., Kamiya, Y. and Choi, G. (2009). Genome-wide analysis of genes targeted by PHYTOCHROME INTERACTING FACTOR 3-LIKE5 during seed germination in Arabidopsis. *Plant Cell* **21**, 403-419.
Okamuro, J. K., den Boer, B. G., Lotys-Prass, C., Szeto, W. and Jofuku, K. D. (1996). Flowers into shoots: photo and hormonal control of a meristem identity switch in Arabidopsis. *Proc. Natl. Acad. Sci. USA* **93**, 13831-13836.
Parcy, F. (2005). Flowering: a time for integration. *Int. J. Dev. Biol.* **49**, 585-593.
Parcy, F., Nilsson, O., Busch, M. A., Lee, I. and Weigel, D. (1998). A genetic framework for floral patterning. *Nature* **395**, 561-566.
Parcy, F., Bomblies, K. and Weigel, D. (2002). Interaction of LEAFY, AGAMOUS and TERMINAL FLOWER1 in maintaining floral meristem identity in Arabidopsis. *Development* **129**, 2519-2527.
Poethig, R. S. (2003). Phase change and the regulation of developmental timing in plants. *Science* **301**, 334-336.
Roux, F., Touzet, P., Cuguen, J. and Le Corre, V. (2006). How to be early flowering: an evolutionary perspective. *Trends Plant Sci.* **11**, 375-381.
Ruiz-Garcia, L., Madueno, F., Wilkinson, M., Haughn, G., Salinas, J. and Martinez-Zapater, J. M. (1997). Different roles of flowering-time genes in the activation of floral initiation genes in Arabidopsis. *Plant Cell* **9**, 1921-1934.
Saddic, L. A., Huvermann, B., Bezhani, S., Su, Y., Winter, C. M., Kwon, C. S., Collum, R. P. and Wagner, D. (2006). The LEAFY target LMI1 is a meristem identity regulator and acts together with LEAFY to regulate expression of CAULIFLOWER. *Development* **133**, 1673-1682.
Sang, Y., Li, Q. H., Rubio, V., Zhang, Y. C., Mao, J., Deng, X. W. and Yang, H. Q. (2005). N-terminal domain-mediated homodimerization is required for photoreceptor activity of Arabidopsis CRYPTOCHROME 1. *Plant Cell* **17**, 1569-1584.
Schmid, M., Uhlenhaut, N. H., Godard, F., Demar, M., Bressan, R., Weigel, D. and Lohmann, J. U. (2003). Dissection of floral induction pathways using global expression analysis. *Development* **130**, 6001-6012.
Schmid, M., Davison, T. S., Henz, S. R., Pape, U. J., Demar, M., Vingron, M., Scholkopf, B., Weigel, D. and Lohmann, J. U. (2005). A gene expression map of Arabidopsis thaliana development. *Nat. Genet.* **37**, 501-506.
Schultz, E. A. and Haughn, G. W. (1993). Genetic analysis of the floral induction process (FLIP) in *Arabidopsis*. *Development* **119**, 745-765.
Shen-Orr, S. S., Milo, R., Mangan, S. and Alon, U. (2002). Network motifs in the transcriptional regulation network of Escherichia coli. *Nat. Genet.* **31**, 64-68.
Shin, R., Burch, A. Y., Huppert, K. A., Tiwari, S. B., Murphy, A. S., Guilfoyle, T. J. and Schachtman, D. P. (2007). The Arabidopsis transcription factor MYB77 modulates auxin signal transduction. *Plant Cell* **19**, 2440-2453.
Sieburth, L. E. and Meyerowitz, E. M. (1997). Molecular dissection of the AGAMOUS control region shows that cis elements for spatial regulation are located intragenically. *Plant Cell* **9**, 355-365.
Simpson, G. G., Gendall, A. R. and Dean, C. (1999). When to switch to flowering. *Annu. Rev. Cell Dev. Biol.* **15**, 519-550.
Smyth, D. R., Bowman, J. L. and Meyerowitz, E. M. (1990). Early flower development in Arabidopsis. *Plant Cell* **2**, 755-767.
Steeves, T. A. and Sussex, I. M. (1989). *Patterns in Plant Development*. Cambridge: Cambridge University Press.
Steffens, N. O., Galuschka, C., Schindler, M., Bulow, L. and Hehl, R. (2004). AthaMap: an online resource for in silico transcription factor binding sites in the Arabidopsis thaliana genome. *Nucleic Acids Res.* **32**, D368-D372.
Stracke, R., Werber, M. and Weisshaar, B. (2001). The R2R3-MYB gene family in Arabidopsis thaliana. *Curr. Opin. Plant Biol.* **4**, 447-456.
Tooke, F., Ordidge, M., Chiurugwi, T. and Battey, N. (2005). Mechanisms and function of flower and inflorescence reversion. *J. Exp. Bot.* **56**, 2587-2599.
Turck, F., Fornara, F. and Coupland, G. (2008). Regulation and identity of florigen: FLOWERING LOCUS T moves center stage. *Annu. Rev. Plant Biol.* **59**, 573-594.
Wagner, D. and Meyerowitz, E. M. (2002). SPLAYED, a novel SWI/SNF ATPase homolog, controls reproductive development in Arabidopsis. *Curr. Biol.* **12**, 85-94.
Wagner, D., Sablowski, R. W. and Meyerowitz, E. M. (1999). Transcriptional activation of APETALA1 by LEAFY. *Science* **285**, 582-584.
Wang, J. W., Czech, B. and Weigel, D. (2009). miR156-regulated SPL transcription factors define an endogenous flowering pathway in Arabidopsis thaliana. *Cell* **138**, 738-749.
Weigel, D., Alvarez, J., Smyth, D. R., Yanofsky, M. F. and Meyerowitz, E. M. (1992). LEAFY controls floral meristem identity in Arabidopsis. *Cell* **69**, 843-859.
Wellmer, F. and Riechmann, J. L. (2010). Gene networks controlling the initiation of flower development. *Trends Genet.* **26**, 519-527.
Wigge, P. A., Kim, M. C., Jaeger, K. E., Busch, W., Schmid, M., Lohmann, J. U. and Weigel, D. (2005). Integration of spatial and temporal information during floral induction in Arabidopsis. *Science* **309**, 1056-1059.
Wilczynski, B. and Furlong, E. E. (2010). Dynamic CRM occupancy reflects a temporal map of developmental progression. *Mol. Syst. Biol.* **6**, 383.
William, D. A., Su, Y., Smith, M. R., Lu, M., Baldwin, D. A. and Wagner, D. (2004). Genomic identification of direct target genes of LEAFY. *Proc. Natl. Acad. Sci. USA* **101**, 1775-1780.
Winter, C. M., Austin, R. S., Blanvillain-Baufume, S., Reback, M. A., Monniaux, M., Wu, M. F., Sang, Y., Yamaguchi, A., Yamaguchi, N., Parker, J. E. et al. (2011). LEAFY target genes reveal floral regulatory logic, cis motifs, and a link to biotic stimulus response. *Dev. Cell* **20**, 430-443.
Xu, M., Hu, T., McKim, S. M., Murmu, J., Haughn, G. W. and Hepworth, S. R. (2010). Arabidopsis BLADE-ON-PETIOLE1 and 2 promote floral meristem fate and determinacy in a previously undefined pathway targeting APETALA1 and AGAMOUS-LIKE24. *Plant J.* **63**, 974-989.
Yamaguchi, A., Kobayashi, Y., Goto, K., Abe, M. and Araki, T. (2005). TWIN SISTER OF FT (TSF) acts as a floral pathway integrator redundantly with FT. *Plant Cell Physiol.* **46**, 1175-1189.
Yamaguchi, A., Wu, M. F., Yang, L., Wu, G., Poethig, R. S. and Wagner, D. (2009). The microRNA-regulated SBP-Box transcription factor SPL3 is a direct upstream activator of LEAFY, FRUITFULL, and APETALA1. *Dev. Cell* **17**, 268-278.
Yu, H., Ito, T., Wellmer, F. and Meyerowitz, E. M. (2004). Repression of AGAMOUS-LIKE 24 is a crucial step in promoting flower development. *Nat. Genet.* **36**, 157-161.
Zhang, Y., Cao, G., Qu, L. J. and Gu, H. (2009). Characterization of Arabidopsis MYB transcription factor gene AtMYB17 and its possible regulation by LEAFY and AGL15. *J. Genet. Genomics* **36**, 99-107.
Zimmermann, I. M., Heim, M. A., Weisshaar, B. and Uhrig, J. F. (2004). Comprehensive identification of Arabidopsis thaliana MYB transcription factors interacting with R/B-like BHLH proteins. *Plant J.* **40**, 22-34.